

A Novel Role for Transcription Factor *Lmo4* in Thymus Development Through Genetic Interaction with *Cited2*

Anna C. Michell, José Bragança[‡], Carol Broadbent, Bradley Joyce, Angela Franklyn, Jürgen E. Schneider, Shoumo Bhattacharya,* and Simon D. Bamforth[†]

Deletion of the transcriptional modulator *Cited2* in the mouse results in embryonic lethality, cardiovascular malformations, adrenal agenesis, cranial ganglia fusion, exencephaly, and left–right patterning defects, all seen with a varying degree of penetrance. The phenotypic heterogeneity, observed on different genetic backgrounds, indicates the existence of both genetic and environmental modifiers. Mice lacking the LIM domain-containing protein *Lmo4* share specific phenotypes with *Cited2* null embryos, such as embryonic lethality, cranial ganglia fusion, and exencephaly. These shared phenotypes suggested that *Lmo4* may be a potential genetic modifier of the *Cited2* phenotype. Examination of *Lmo4*-deficient embryos revealed partially penetrant cardiovascular malformations and hypoplastic thymus. Examination of *Lmo4*;*Cited2* compound mutants indicated that there is a genetic interaction between *Cited2* and *Lmo4* in control of thymus development. Our data suggest that this may occur, in part, through control of expression of a common target gene, *Tbx1*, which is necessary for normal thymus development. *Developmental Dynamics* 239:1988–1994, 2010. © 2010 Wiley-Liss, Inc.

Key words: *Cited2*; *Lmo4*; thymus development; *Tbx1*; modifiers

Accepted 29 April 2010

INTRODUCTION

The transcription factor CITED2, which binds CREBBP with high affinity (Bhattacharya et al., 1999), acts as a co-factor for transcription factors such as TFAP2, LHX2, PPARA, and SMAD2/3 (Glenn and Maurer, 1999; Braganca et al., 2003; Tien et al., 2004; Chou and Yang, 2006), as well as acting as a repressor of hypoxia-activated transcription (Bhattacharya et al., 1999). Mice null for *Cited2* die

in utero from phenotypically heterogeneous cardiac malformations including atrial, ventricular, and atrioventricular septal defects (ASD, VSD, AVSD); outflow tract defects (double-outlet right ventricle [DORV], common arterial trunk [CAT], tetralogy of Fallot [TOF], transposition of great arteries [TGA]); and interrupted and right-sided aortic arch (Bamforth et al., 2001, 2004; Yin et al., 2002; Weninger et al., 2005). Loss of *Cited2* also gives rise to exen-

cephaly, cranial ganglia fusion, abnormal migration of cardiac neural crest cells, absent adrenal glands, and placental abnormalities (Bamforth et al., 2001, 2004; Barbera et al., 2002; Yin et al., 2002; Weninger et al., 2005; Withington et al., 2006; Val et al., 2007). On a congenic C57Bl/6J background, *Cited2*-null mice show left–right patterning defects characterized by right atrial and pulmonary isomerism, and abnormal ventricular topology (Bamforth et al., 2004; Weninger

Additional Supporting Information may be found in the online version of this article.

Department of Cardiovascular Medicine, Wellcome Trust Centre for Human Genetics, University of Oxford, Roosevelt Drive, Oxford, United Kingdom

[†]Dr. Bamforth's present address is Institute of Human Genetics, Newcastle University, Centre for Life, Central Parkway, Newcastle upon Tyne, NE1 3BZ, UK.

[‡]Dr. Bragança's present address is Institute for Biotechnology and Bioengineering, Centre for Molecular and Structural Biomedicine (CBME), University of Algarve, 8005-139 Faro, Portugal

Grant sponsor: Wellcome Trust Program Grant; Grant number: 083228; Grant sponsor: Wellcome Trust Program Core Grant; Grant number: 075491/Z/04; Grant sponsor: British Heart Foundation DPhil Studentship; Grant number: FS/05/121.

*Correspondence to: Shoumo Bhattacharya, Department of Cardiovascular Medicine, Wellcome Trust Centre for Human Genetics, University of Oxford, Roosevelt Drive, Oxford, OX3 7BN, UK. E-mail: sbhattac@well.ox.ac.uk

DOI 10.1002/dvdy.22334

Published online 28 May 2010 in Wiley InterScience (www.interscience.wiley.com).

et al., 2005). We have recently shown that the phenotypically heterogeneous and penetrant cardiac malformations in *Cited2* deficiency arise from a primary requirement in epiblast derivatives for left–right patterning, with a secondary cell-autonomous role in the mesoderm (MacDonald et al., 2008).

Cited2 binds the LIM homeodomain transcription factor, *Lhx2*, by means of LIM domains (Glenn and Maurer, 1999). Proteins containing LIM domains function as transcriptional regulators, and this domain may act as a molecular adaptor for multiprotein complexes. The subfamily of LIM-only (LMO) proteins comprises four members (*Lmo1*–*Lmo4*). These non-DNA binding transcription factors may affect transcription by protein–protein interaction with DNA-binding transcription factors or chromatin modeling proteins (Hahm et al., 2004). *Lmo4* comprises two zinc-binding LIM domains and is widely expressed in the developing embryo, including the pharyngeal arches, thymus, and neural crest (Grutz et al., 1998; Kenny et al., 1998; Sugihara et al., 1998). Mouse embryos lacking *Lmo4* display a phenotype that overlaps with *Cited2*^{−/−} embryos. This includes exencephaly, in utero or perinatal lethality, and cranial nerve fusions (Hahm et al., 2004; Tse et al., 2004; Lee et al., 2005).

The shared specific phenotypes observed in *Cited2* and *Lmo4* mutant mice suggest that there may be a genetic interaction. In this study, we show that embryos lacking *Lmo4* have partially penetrant cardiac malformations including VSD, DORV, and right-sided aortic arch, which have not previously been reported. The shared specific phenotypes are further extended by demonstrating cervical fusions and abnormal thymus in *Cited2* and in *Lmo4* mutant embryos. The thymus is significantly smaller in compound mutant embryos, and completely absent in embryos lacking both *Lmo4* and *Cited2*, indicating that there is a genetic interaction. Expression of *Tbx1*, which is important for thymus development, was significantly reduced in *Lmo4* and *Cited2* mutant embryos. This suggests a novel role for *Cited2* and *Lmo4* acting, likely in

part through *Tbx1*, to control development of the thymus.

RESULTS

Cervical Vertebrae

Abnormalities in *Cited2*^{−/−} Embryos

Lmo4^{−/−} embryos show homeotic-like transformations in the rib cage and cervical vertebrae, although at low penetrance (Hahm et al., 2004). To investigate whether similar defects were present in the *Cited2*^{−/−} embryos, skeletal preparations were made at embryonic day (E) 17.5. This revealed that *Cited2*^{−/−} embryos (on a mixed genetic background) have fusions of the cervical vertebrae (Fig. 1). The cervical vertebrae may be completely fused (Fig. 1c,d) from the exoccipital bone through to the atlas (C1), axis (C2), and the third cervical vertebra (C3). Less severe fusions are also observed, which may even be asymmetric (Fig. 1c). The cervical skeleton from one of the less severely affected *Cited2*^{−/−} embryos was disarticulated revealing an anterior transformation (Fig. 1g,h). The axis had a structure resembling the anterior arch of the atlas, and the atlas was missing this. The rib cages, however, were unaffected. Similar cervical vertebrae fusions were also observed in embryos on congenic 129Sv and C57Bl/6J genetic backgrounds (data not shown).

Cardiovascular Defects and Thymus Hypoplasia in *Lmo4*^{−/−} Embryos

Cardiovascular defects, a major aspect of the *Cited2* phenotype, have not been reported in *Lmo4* mutant mice. We therefore investigated whether the *Lmo4*^{−/−} embryos suffered from any cardiac developmental abnormalities. Heterozygous *Lmo4* mice (Tse et al., 2004) were intercrossed to analyze embryos at E15.5 by magnetic resonance imaging (MRI). Gross external analysis of *Lmo4*^{−/−} embryos showed exencephaly (2/8; data not shown), as previously reported (Hahm et al., 2004; Tse et al., 2004; Lee et al., 2005), and edema (2/8; data not shown). Analysis by MRI revealed incomplete pene-

trance of cardiovascular defects in *Lmo4*^{−/−} embryos, including VSD with DORV (2/8) and a right-sided aortic arch (1/8; Fig. 2).

Lmo4^{−/−} embryos also had consistently hypoplastic thymuses (8/8) compared with wild-type littermates which, in some cases, were malpositioned (3/8, Fig. 3b,d). Volume calculations showed a significant 2.3-fold decrease between wild-type (n = 6) and *Lmo4*^{−/−}, thymuses (n = 8; *P* < 0.0005; Fig. 3e). Thymuses of *Lmo4*^{+/−} littermates were not significantly different to those of wild-type littermates (n = 7; data not shown). Thymus size in *Cited2*^{−/−} embryos at E15.5 was then assessed to see if they were affected. A significant 1.6-fold decrease in thymus volume was found (n = 6 wild-type, n = 6 *Cited2*^{−/−}; *P* < 0.001; Fig. 3f). We also measured adrenal gland volume, because *Cited2*^{−/−} embryos exhibit adrenal agenesis (Bamforth et al., 2001). However, we did not find any significant reduction in the size of adrenal glands in *Lmo4*^{−/−} embryos compared with those of wild-type littermates (n = 6 for each genotype; data not shown).

Cited2 and *Lmo4* Genetically Interact In Vivo

As *Cited2* and *Lmo4* mutant mice share several specific phenotypes, we tested whether there was a genetic interaction in vivo by intercrossing *Lmo4*^{+/−} mice with *Cited2*^{+/−} mice (Supp. Table S1, which is available online). As *Lmo4*^{+/−};*Cited2*^{+/−} mice were viable, we intercrossed them to produce compound and double knockout mice. Mice null for either *Cited2* or *Lmo4* were not present at weaning, as expected (Supp. Table S2). Embryos from *Lmo4*^{+/−};*Cited2*^{+/−} intercrosses were collected at E15.5 and examined by MRI (n = 141). Supplementary Table S3 and Supp. Figures S1 and S2 summarize the defects observed in these embryos, the genotypes of which were all present in normal Mendelian ratios at this point in gestation. We observed no significant differences in the incidence of cardiovascular malformations in the compound heterozygous/knockout or double knockout embryos. Spina bifida was occasionally observed in embryos of the same genotype that exhibited

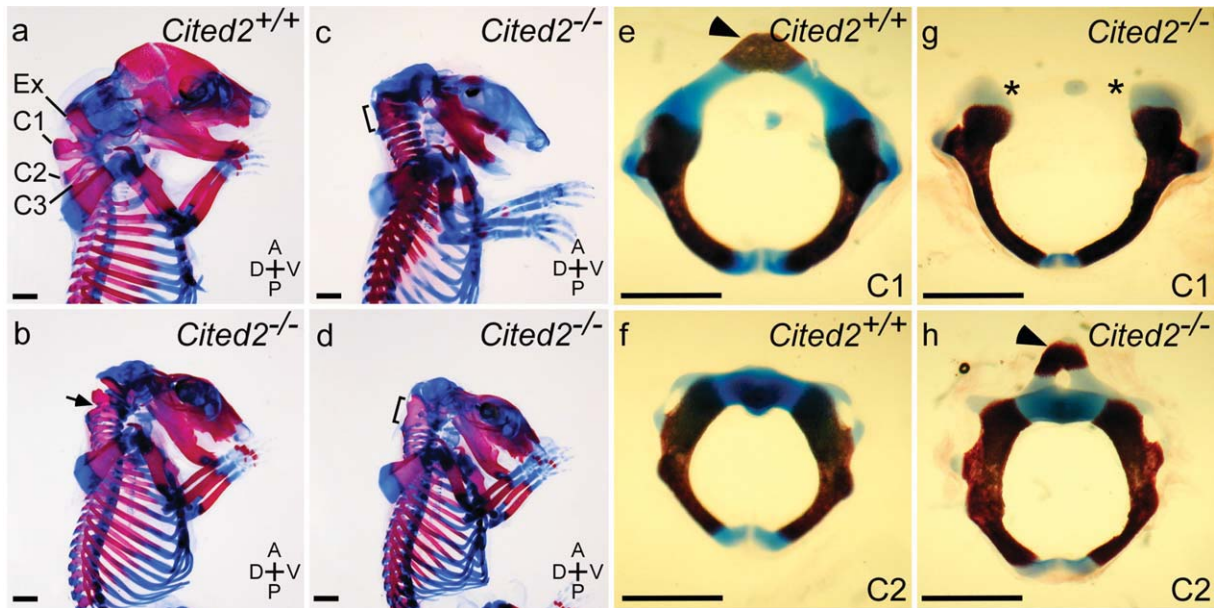


Fig. 1. Skeletal defects in embryonic day (E) 17.5 *Cited2*^{-/-} embryos. **a:** Wild-type (*Cited2*^{+/+}) embryo skeleton showing the normal appearance of the cervical vertebrae. **b–d:** *Cited2*^{-/-} skeletons showing various degrees of fusion between the cervical vertebrae (indicated). All embryos depicted had exencephaly and are missing the occipital and frontal skull bones. **e–h:** Disarticulated cervical vertebrae from a *Cited2*^{-/-} skeleton with less severe fusions. **e:** Wild-type atlas, with anterior arch indicated (arrowhead). **f:** Wild-type axis. **g:** *Cited2*^{-/-} atlas which is missing the anterior arch (asterisks). **h:** *Cited2*^{-/-} axis, which has a structure resembling the anterior arch of the atlas (arrowhead). Ex, exoccipital; C1, atlas; C2, axis. Scale bar = 1 mm.

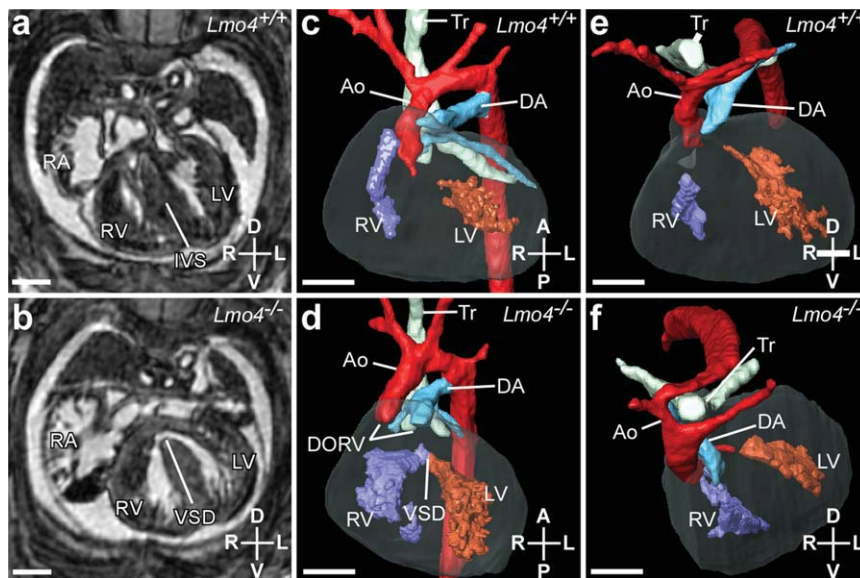


Fig. 2. Cardiovascular defects observed in embryonic day (E) 15.5 *Lmo4*^{-/-} embryos. **a,b:** Transverse magnetic resonance imaging sections of wild-type (a) and *Lmo4*^{-/-} (b) embryo hearts. A ventricular septal defect (VSD) is visible in the *Lmo4*^{-/-} heart. **c–f:** Three-dimensional reconstructions of embryo hearts and great vessels. **c,d:** Ventral views of wild-type embryo heart (c) showing normal topology, and *Lmo4*^{-/-} embryo heart (d) showing a VSD and double-outlet right ventricle (DORV), where both the aorta (Ao) and ductus arteriosus (DA) arise from the right ventricle (RV). **e,f:** Anterior views of wild-type embryo heart (e) showing normal topology, and *Lmo4*^{-/-} embryo heart (f) showing a right-sided aortic arch and ductus arteriosus. RA, right atrium; LA, left atrium; LV, left ventricle; IVS, intra-ventricular septum; PA, pulmonary arteries; Tr, trachea. Scale bar = 500 μ m.

exencephaly (Supp. Fig. 1), a phenotype not described before for either *Lmo4* or *Cited2* mutant embryos.

Although cardiovascular development did not seem to be affected by *Lmo4* and *Cited2* epistasis, the thy-

mus was absent in *Lmo4*^{-/-};*Cited2*^{-/-} embryos. Thymus defects were observed in most *Lmo4*;*Cited2* compound mutant genotypes (Supp. Table S3), including thymus hypoplasia, separated thymus lobes, and one lobe absent (Fig. 4a,b). A single *Lmo4*^{-/-};*Cited2*^{+/+} embryo was also lacking both thymus lobes. Thymuses from representative embryos of all genotypes were compared by volume ($n = 5$ each genotype; Fig. 4c). No significant difference was found between the thymuses of *Lmo4*^{+/+};*Cited2*^{+/+}, *Lmo4*^{+/+};*Cited2*^{+/-} or *Lmo4*^{+/-};*Cited2*^{+/-} embryos when compared with thymuses from wild-type embryos. The thymuses of *Lmo4*^{-/-};*Cited2*^{+/+} ($P = 0.0005$) and *Lmo4*^{+/+};*Cited2*^{-/-} ($P = 0.0198$) embryos were significantly reduced compared with those of wild-type embryos. Further loss of one copy of *Lmo4* reduced the average thymus volume in *Lmo4*^{+/+};*Cited2*^{-/-} embryos compared with *Lmo4*^{+/+};*Cited2*^{-/-} embryos ($P = 0.0187$), but thymuses of *Lmo4*^{-/-};*Cited2*^{+/-} embryos, when present, were not significantly smaller than in *Lmo4*^{-/-};*Cited2*^{+/+} embryos.

The complete lack of thymus in *Lmo4*^{-/-};*Cited2*^{-/-} embryos is a novel phenotype, not previously seen in either individual knockout. This

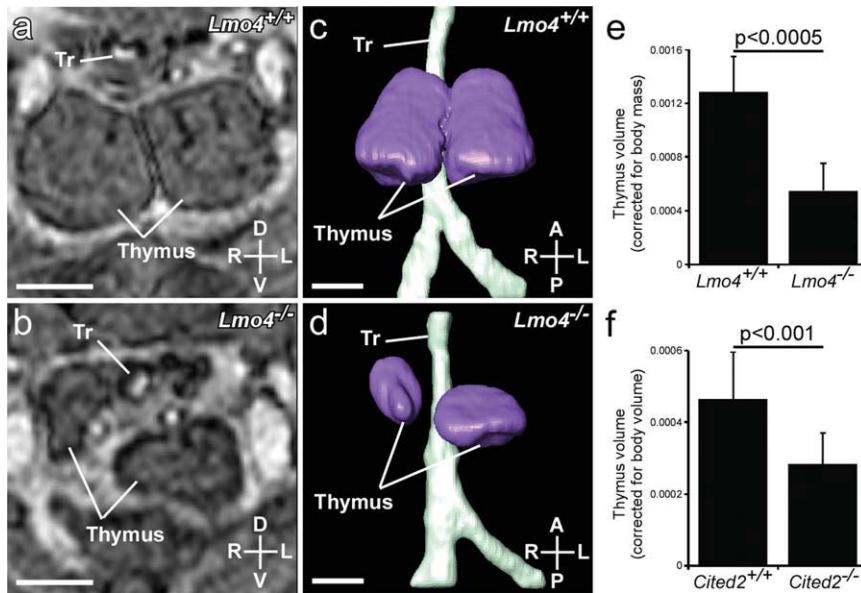


Fig. 3. Thymus hypoplasia and malpositioning observed in embryonic day (E) 15.5 *Lmo4*^{-/-} embryos. **a,b:** Transverse magnetic resonance imaging (MRI) sections of the thymus of wild-type (*Lmo4*^{+/+}; **a**) and *Lmo4*^{-/-} (**b**) littermate embryos. **c,d:** Three-dimensional (3D) reconstructions (ventral view) of thymus and trachea showing normal position and equal-sized lobes from wild-type (**c**) and hypoplasia, abnormal positioning and separation of the lobes in a *Lmo4*^{-/-} embryo (**d**). **e:** Thymus volumes from *Lmo4*^{+/+} and *Lmo4*^{-/-} embryos, corrected for embryo mass. **f:** Thymus volumes from *Cited2*^{+/+} and *Cited2*^{-/-} embryos, corrected for whole embryo volume. (Graph values are means \pm SD). Scale bar = 500 μ m.

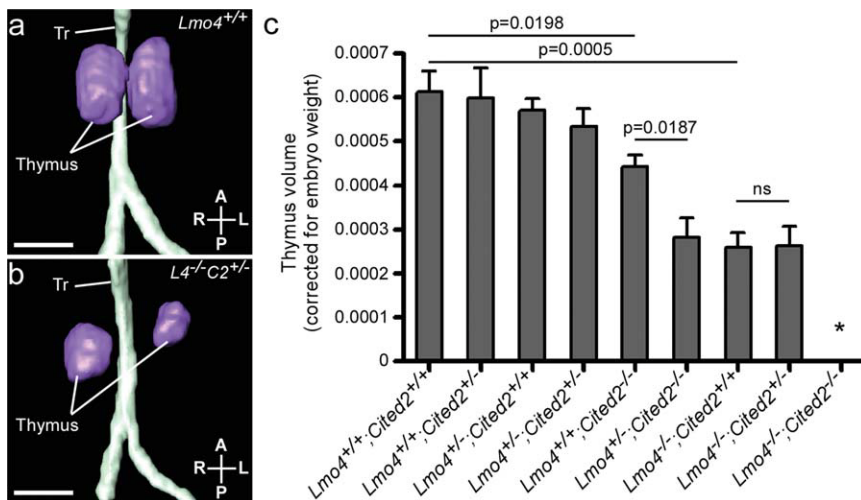


Fig. 4. Impaired thymus development in *Lmo4* and *Cited2* compound mutant embryos. **a,b:** Three-dimensional (3D) reconstruction of thymuses from embryonic day (E) 15.5 embryos by MRI. **a:** Thymus and trachea from a wild-type (*Lmo4*^{+/+}) embryo, showing normal position and equal-sized lobes. **b:** *Lmo4*^{-/-};*Cited2*^{+/-} thymus illustrating hypoplasia, abnormal positioning, and separation of the lobes. **c:** Comparison of whole thymus volumes, adjusted for embryo weight, in embryos of all possible genotypes from *Lmo4*^{+/+};*Cited2*^{+/-} intercrosses (Mean \pm SEM). *Lmo4*^{-/-};*Cited2*^{-/-} embryos do not have a thymus (*). Scale bar = 500 μ m.

indicates that *Cited2* and *Lmo4* interact to control thymus development. To investigate whether there is a common target for *Cited2* and *Lmo4*, embryos were harvested for quantitative reverse transcriptase-polymerase

chain reaction (QRT-PCR) analysis. Pharyngeal arches and hearts were dissected from E10.5 *Cited2*^{-/-} and *Lmo4*^{-/-} embryos. Expression of *Cited2* and *Lmo4*, as well as potential target candidate genes, *Pitx2c* and

Tbx1, were investigated. *Pitx2c* was selected as it is a known target of *Cited2* (Bamforth et al., 2004), and *Tbx1* was selected as it has been implicated in thymus development (Jerome and Papaioannou, 2001).

Tbx1 Expression in *Cited2*^{-/-} and *Lmo4*^{-/-} Embryos

Gene expression levels were analyzed from the dissected hearts and pharyngeal arches of E10.5 embryos. *Cited2*^{-/-} embryos showed a modest yet highly significant decrease in levels of *Lmo4* mRNA when compared with wild-type littermates (1.35-fold decrease; $P = 0.00006$, $n = 12$ *Cited2*^{+/+} vs. $n = 12$ *Cited2*^{-/-} embryos), but *Lmo4*^{-/-} embryos did not show any difference in *Cited2* levels ($n = 12$ *Lmo4*^{+/+} vs. $n = 12$ *Lmo4*^{-/-} embryos; Fig. 5a,b), indicating that *Lmo4* is downstream of *Cited2*. As we have previously shown (MacDonald et al., 2008), *Cited2*^{-/-} embryos have lower levels of *Pitx2c* mRNA, compared with wild-type littermates (1.43-fold decrease, $P = 0.01$; Fig. 5c), but *Lmo4*^{-/-} embryos did not show any difference in *Pitx2c* levels ($n = 12$ embryos for each genotype tested; Fig. 5d). *Tbx1* levels were then investigated in the dissected pharyngeal arch regions from E10.5 *Cited2*^{-/-} and *Lmo4*^{-/-} embryos. A significant decrease in *Tbx1* levels was found in both *Cited2*^{-/-} (1.46-fold decrease, $p = 0.009$) and *Lmo4*^{-/-} (2.3-fold decrease; $P = 0.018$, $n = 12$ embryos for each genotype tested; Fig. 5e,f). This suggests that *Tbx1* could be a common target for *Cited2* and *Lmo4* in the developing pharyngeal arches.

DISCUSSION

Genetic interactions can be identified through screens testing pairwise combinations of mutant genes that either suppress or enhance the original mutant phenotype (Hartman et al., 2001). In pairwise intervention experiments, the expected outcome of a double-intervention is the product of the two single-intervention effects; departure from this model indicates a functional relationship (i.e., either an aggravating or an alleviating effect, indicating compensatory function or gene-action in series, respectively) between the two

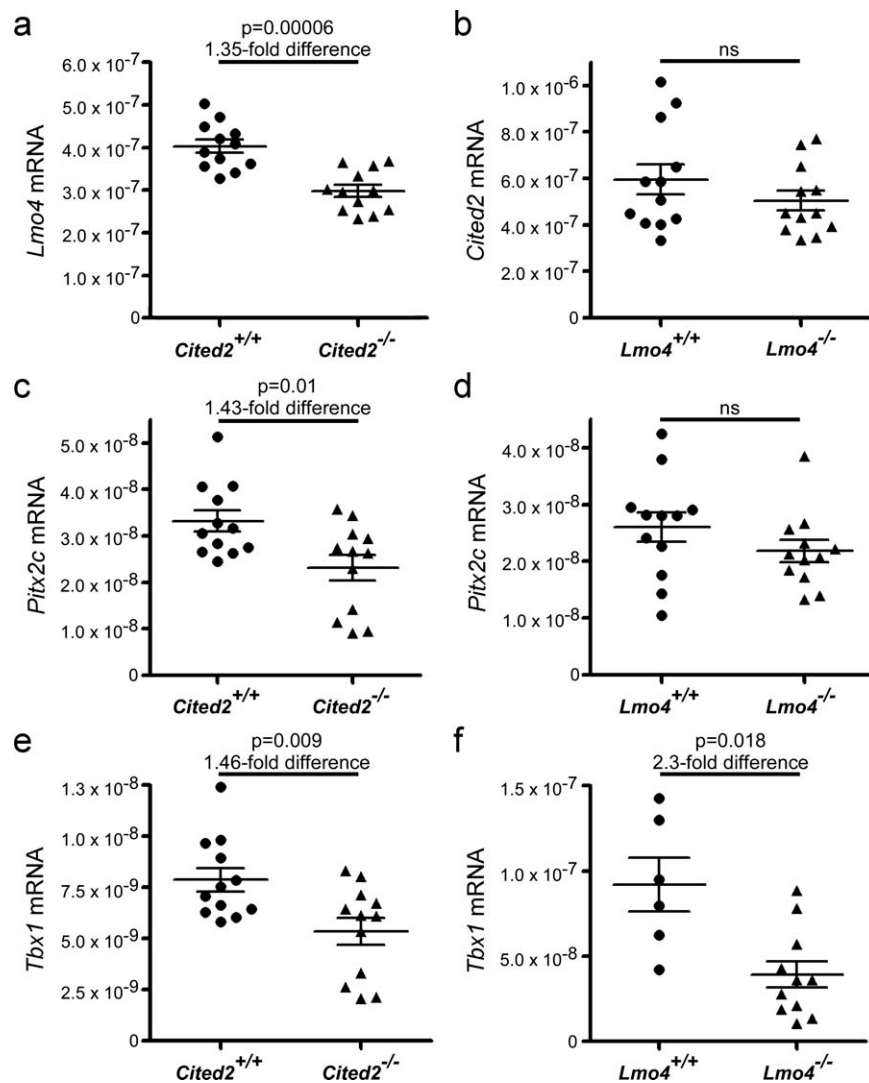


Fig. 5. mRNA expression in embryos lacking *Cited2* or *Lmo4*. Quantitative reverse transcriptase-polymerase chain reaction was conducted on pharyngeal arches and hearts harvested from embryonic day (E) 10.5 *Cited2*^{+/+}, *Cited2*^{-/-}, *Lmo4*^{+/+} and *Lmo4*^{-/-} embryos. **a:** *Lmo4* expression is significantly decreased in *Cited2*^{-/-} embryos. **b:** *Cited2* expression was not affected in *Lmo4*^{-/-} embryos. **c,d:** *Pitx2c* expression was significantly decreased in *Cited2*^{-/-} embryos (c) but was not affected in *Lmo4*^{-/-} embryos (d). **e,f:** *Tbx1* expression was reduced in *Cited2*^{-/-} embryos (e) and in *Lmo4*^{-/-} embryos (f). Mean \pm SEM are indicated.

target genes (St Onge et al., 2007). This approach has been used in *Drosophila melanogaster* and *Caenorhabditis elegans* to identify genes acting in the same pathway (Lehner et al., 2006; Sambandan et al., 2008). Also, genes that share similar or identical GO term annotations are more likely to interact genetically, as shown by the analysis of thousands of mutant *Saccharomyces cerevisiae* yeast strains (Wong et al., 2004). This is also true for genes that encode proteins found in the same subcellular location, or that act in the same protein complex. Another excellent predictor of a genetic interaction is a

shared specific mutant phenotype (Tong et al., 2004). Mouse embryos lacking *Cited2* or *Lmo4* share specific phenotypes, both displaying exencephaly and cardiovascular, thymus, skeletal, and cranial ganglia defects. Experiments to identify a genetic interaction revealed that *Lmo4*^{-/-}; *Cited2*^{-/-} embryos completely lacked a thymus, a novel phenotype, not observed in either parental line. However, there was no significant increase in penetrance of cardiac malformation in *Lmo4*^{-/-}; *Cited2*^{-/-} embryos.

As discussed by Wong et al., a genetic interaction between two genes

is indicated when the phenotype observed is more pronounced than the phenotype produced by the genes individually (Wong et al., 2004). Having re-analyzed previously published studies, Mani et al. (2008) concluded that the expected phenotype in offspring should be the product of the parental fitness, and not the average of parental fitness or that of the least fit parent as previously thought (Tong et al., 2001, 2004). This allows for greater expected deviation from parental fitness in offspring. For instance, if one parent had a fitness of 0.6 and one a fitness of 0.8, the expected fitness of the offspring is not 0.7 (average) or 0.6 (least fit parent), but 0.48 (product). Thus, applying this principle to these results, where *Lmo4*^{-/-} embryos had thymuses 0.46 times the size of wild-type thymuses, and *Cited2*^{-/-} thymuses were 0.78 times the size of wild-type thymuses, the expected thymus size of *Lmo4*^{-/-}; *Cited2*^{-/-} embryos should be 0.36 times the size of those in wild-type embryos. However, a total lack of thymus was discovered, dramatically exceeding the expected decrease. This indicates that a genetic interaction between *Lmo4* and *Cited2* is necessary for thymus development, suggesting that the genes act together in a common developmental process or molecular target.

Pitx2c is a known target of *Cited2*, but QRT-PCR data showed that it is not a target of *Lmo4*. Nor is *Cited2* a target of *Lmo4*, although it appears that *Lmo4* could be a target of *Cited2*. The data also revealed that *Tbx1* expression levels are reduced in response to loss of both *Cited2* and *Lmo4* expression. This could indicate that *Tbx1* is a common target of *Cited2* and *Lmo4*, all of which are necessary for normal thymus formation. Indeed, Ivins et al. identified a reduction in *Lmo4* expression in embryos lacking *Tbx1* expression at E9.5 (Ivins et al., 2005). *Tbx1* is expressed in the developing pharyngeal endoderm, which contributes to thymus formation. Absent thymus is a feature of DiGeorge / 22q11 deletion syndrome (Lischner, 1972; de la Chapelle et al., 1981), for which the majority of phenotypes observed are largely attributed to haploinsufficiency of *TBX1* during development

(Chieffo et al., 1997; Jerome and Papaioannou, 2001; Lindsay and Baldini, 2001). Moreover, in the mouse, morphology of the thymus is sensitive to *Tbx1* dosage (Zhang and Baldini, 2007). *Lmo4* is strongly expressed in the pharyngeal arches during mouse embryonic development (Hahm et al., 2004), specifically in the migratory cranial neural crest, and highly expressed in proliferating T lymphocytes in adult thymus (Kenny et al., 1998). *Cited2* is also strongly expressed in the pharyngeal arches during development, in endoderm, mesenchyme and ectoderm (Weninger et al., 2005; MacDonald et al., 2008), and it is the third pharyngeal pouch from which the thymus is derived. The expression of *Tbx1* in the fourth pharyngeal arch is also important for normal formation of the fourth pharyngeal arch arteries (Lischner, 1972; Jerome and Papaioannou, 2001), the development of which are affected in embryos lacking *Cited2* and/or *Lmo4*.

Our data show that *Lmo4*^{-/-} embryos have incomplete penetrance of cardiovascular defects in addition to those phenotypes already known, which has not been previously reported. Thymus defects have also not been previously reported and were detected by MRI, despite Tse et al. (2004) noting a normal cellular architecture of the thymus from histological sections, and no hypoplasia was recorded (Tse et al., 2004). Adding cardiovascular and thymus defects to the list of similarities between the recorded phenotypes of both *Cited2* and *Lmo4* knockout mice gave strong grounds for a physical and genetic interaction between *Cited2* and *Lmo4*. Indeed, using GST pull-down assays, we were able to show that LMO4 physically interacts with residues 123–161 of CITED2, although we were unable to co-immunoprecipitate *Lmo4* and *Cited2* (data not shown).

To fully understand the genetic network in which *Cited2*, *Lmo4*, and *Tbx1* are potentially interacting to control thymus development, further experiments will need to be performed. Although QRT-PCR data gives a quantitative measure of altered expression, qualitative assays will be needed to complement this, for example, by using in situ hybridization techniques to investigate whether the expression

of *Tbx1* is reduced specifically in the endoderm as may be expected. A more detailed investigation of candidate genes in wild-type and double heterozygote embryos and double homozygous null embryos will also need to be carried out, looking at the expression profile of genes specifically expressed in thymus such as *Foxn1* (Nehls et al., 1996), and those expressed in the pharyngeal arches and known to affect thymus development, for example, *Pax9*, *Eya1*, and *Six1* (Peters et al., 1998; Xu et al., 2002; Zou et al., 2006).

To summarize, in this study we have shown that mice lacking *Lmo4* exhibit cardiovascular and thymus defects, which are novel phenotypes and add *Lmo4* to the genetic network involved in cardiovascular development. *Lmo4* interacts genetically with *Cited2* in vivo to control thymus development, possibly through a common target gene in *Tbx1*.

EXPERIMENTAL PROCEDURES

Mice

Cited2^{+/-} mice (*Cited2*^{tm1Bha}) on a mixed or congenic C57BL/6J background (Bamforth et al., 2001, 2004) and *Lmo4*^{+/-} mice (gift from T. Rabbitts, LMB Cambridge; Tse et al., 2004) were used in this study. Embryos were harvested at the indicated time points after detection of a vaginal plug (E0.5), and genotyped using allele-specific PCR (primer details are available on request). All animal experimentation was performed under UK Home Office authorization and regulations.

Imaging

Magnetic resonance imaging was performed on a horizontal 9.4T/21cm VNMRs Direct Drive MR system (Varian Inc., Palo Alto) essentially as described previously (Schneider et al., 2004) on embryos at E15.5. Skeletons were prepared and stained with alizarin red (bone) and Alcian blue (cartilage) by standard methods.

QRT-PCR

The hearts and pharyngeal arch regions were dissected free from E10.5 embryos as described (Prescott et al.,

2005). RNA isolation, cDNA synthesis, and quantitative RT-PCR (QRT-PCR) reactions were carried out as described (MacDonald et al., 2008) using preoptimized TaqMan primer-probe sets from Applied Biosystems (*Mus musculus* assays Mm00516121_m1 (NM_010828 *Cited2*), Mm00495373_m1 (NM_010723 *Lmo4*), Mm00440826_m1 (NM_001042502 *Pitx2c*), Mm00448948_m1 (NM_011532 *Tbx1*), and eukaryotic 18S rRNA. Expression levels were normalized to 18S rRNA using the R₀ method of analysis (Peirson et al., 2003).

Statistical Analyses

The chi-squared test was used to calculate the deviation from expected Mendelian ratios. QRT-PCR data was analyzed using a two-tailed, two-sample *t*-test assuming unequal variance.

ACKNOWLEDGMENTS

We thank T. Rabbitts for *Lmo4* mice. A.C.M is the recipient of a British Heart Foundation DPhil Studentship. S.B. is supported by a British Heart Foundation Chair Award [CH/09/003]. This work was funded by Wellcome Trust Program Grant Award [083228] to S.B., and by a Wellcome Trust Core Grant Award [075491/Z/04].

REFERENCES

- Bamforth SD, Braganca J, Eloranta JJ, Murdoch JN, Marques FI, Kranc KR, Farza H, Henderson DJ, Hurst HC, Bhattacharya S. 2001. Cardiac malformations, adrenal agenesis, neural crest defects and exencephaly in mice lacking *Cited2*, a new Tfap2 co-activator. *Nat Genet* 29:469–474.
- Bamforth SD, Braganca J, Farthing CR, Schneider JE, Broadbent C, Michell AC, Clarke K, Neubauer S, Norris D, Brown NA, Anderson RH, Bhattacharya S. 2004. *Cited2* controls left-right patterning and heart development through a Nodal-*Pitx2c* pathway. *Nat Genet* 36: 1189–1196.
- Barbera JP, Rodriguez TA, Greene ND, Weninger WJ, Simeone A, Copp AJ, Beddington RS, Dunwoodie S. 2002. Folic acid prevents exencephaly in *Cited2* deficient mice. *Hum Mol Genet* 11: 283–293.
- Bhattacharya S, Michels CL, Leung MK, Arany ZP, Kung AL, Livingston DM. 1999. Functional role of p35srj, a novel p300/CBP binding protein, during transactivation by HIF-1. *Genes Dev* 13:64–75.

- Braganca J, Eloranta JJ, Bamforth SD, Ibbitt JC, Hurst HC, Bhattacharya S. 2003. Physical and functional interactions among AP-2 transcription factors, p300/CREB-binding protein, and CITED2. *J Biol Chem* 278:16021–16029.
- Chieffo C, Garvey N, Gong W, Roe B, Zhang G, Silver L, Emanuel BS, Budarf ML. 1997. Isolation and characterization of a gene from the DiGeorge chromosomal region homologous to the mouse Tbx1 gene. *Genomics* 43:267–277.
- Chou YT, Yang YC. 2006. Post-transcriptional control of Cited2 by transforming growth factor beta. Regulation via Smads and Cited2 coding region. *J Biol Chem* 281:18451–18462.
- de la Chapelle A, Herva R, Koivisto M, Aula P. 1981. A deletion in chromosome 22 can cause DiGeorge syndrome. *Hum Genet* 57:253–256.
- Glenn DJ, Maurer RA. 1999. MRG1 binds to the LIM domain of Lhx2 and may function as a coactivator to stimulate glycoprotein hormone alpha-subunit gene expression. *J Biol Chem* 274:36159–36167.
- Grutz G, Forster A, Rabbitts TH. 1998. Identification of the LMO4 gene encoding an interaction partner of the LIM-binding protein LDB1/NLI1: a candidate for displacement by LMO proteins in T cell acute leukaemia. *Oncogene* 17:2799–2803.
- Hahn K, Sum EY, Fujiwara Y, Lindeman GJ, Visvader JE, Orkin SH. 2004. Defective neural tube closure and anteroposterior patterning in mice lacking the LIM protein LMO4 or its interacting partner Deaf-1. *Mol Cell Biol* 24:2074–2082.
- Hartman JL, IV, Garvik B, Hartwell L. 2001. Principles for the buffering of genetic variation. *Science* 291:1001–1004.
- Ivins S, Lammerts van Beuren K, Roberts C, James C, Lindsay E, Baldini A, Ataliotis P, Scambler PJ. 2005. Microarray analysis detects differentially expressed genes in the pharyngeal region of mice lacking Tbx1. *Dev Biol* 285:554–569.
- Jerome LA, Papaioannou VE. 2001. DiGeorge syndrome phenotype in mice mutant for the T-box gene, Tbx1. *Nat Genet* 27:286–291.
- Kenny DA, Jurata LW, Saga Y, Gill GN. 1998. Identification and characterization of LMO4, an LMO gene with a novel pattern of expression during embryogenesis. *Proc Natl Acad Sci U S A* 95:11257–11262.
- Lee SK, Jurata LW, Nowak R, Lettieri K, Kenny DA, Pfaff SL, Gill GN. 2005. The LIM domain-only protein LMO4 is required for neural tube closure. *Mol Cell Neurosci* 28:205–214.
- Lehner B, Crombie C, Tischler J, Fortunato A, Fraser AG. 2006. Systematic mapping of genetic interactions in *Caenorhabditis elegans* identifies common modifiers of diverse signaling pathways. *Nat Genet* 38:896–903.
- Lindsay EA, Baldini A. 2001. Recovery from arterial growth delay reduces penetrance of cardiovascular defects in mice deleted for the DiGeorge syndrome region. *Hum Mol Genet* 10:997–1002.
- Lischner HW. 1972. DiGeorge syndrome(s). *J Pediatr* 81:1042–1044.
- MacDonald ST, Bamforth SD, Chen CM, Farthing CR, Franklyn A, Broadbent C, Schneider JE, Saga Y, Lewandoski M, Bhattacharya S. 2008. Epiblastic Cited2 deficiency results in cardiac phenotypic heterogeneity and provides a mechanism for haploinsufficiency. *Cardiovasc Res* 79:448–457.
- Mani R, St. Onge RP, Hartman JL, Giaever G, Roth FP. 2008. Defining genetic interaction. *Proc Natl Acad Sci U S A* 105:3461–3466.
- Nehls M, Kyewski B, Messerle M, Waldschutz R, Schuddekopf K, Smith AJ, Boehm T. 1996. Two genetically separable steps in the differentiation of thymic epithelium. *Science* 272:886–889.
- Peirson SN, Butler JN, Foster RG. 2003. Experimental validation of novel and conventional approaches to quantitative real-time PCR data analysis. *Nucleic Acids Res* 31:e73.
- Peters H, Neubuser A, Kratochwil K, Balling R. 1998. Pax9-deficient mice lack pharyngeal pouch derivatives and teeth and exhibit craniofacial and limb abnormalities. *Genes Dev* 12:2735–2747.
- Prescott K, Ivins S, Hubank M, Lindsay E, Baldini A, Scambler P. 2005. Microarray analysis of the Df1 mouse model of the 22q11 deletion syndrome. *Hum Genet* 116:486–496.
- Sambandan D, Carbone MA, Anholt RRH, Mackay TFC. 2008. Phenotypic plasticity and genotype by environment interaction for olfactory behavior in *Drosophila melanogaster*. *Genetics* 179:1079–1088.
- Schneider JE, Bose J, Bamforth SD, Gruber AD, Broadbent C, Clarke K, Neubauer S, Lengeling A, Bhattacharya S. 2004. Identification of cardiac malformations in mice lacking Ptdsr using a novel high-throughput magnetic resonance imaging technique. *BMC Dev Biol* 4:16.
- St Onge RP, Mani R, Oh J, Proctor M, Fung E, Davis RW, Nislow C, Roth FP, Giaever G. 2007. Systematic pathway analysis using high-resolution fitness profiling of combinatorial gene deletions. *Nat Genet* 39:199–206.
- Sugihara TM, Bach I, Kioussi C, Rosenfeld MG, Andersen B. 1998. Mouse deformed epidermal autoregulatory factor 1 recruits a LIM domain factor, LMO-4, and CLIM coregulators. *Proc Natl Acad Sci U S A* 95:15418–15423.
- Tien ES, Davis JW, Vanden Heuvel JP. 2004. Identification of the CREB-binding protein/p300-interacting protein CITED2 as a peroxisome proliferator-activated receptor alpha coregulator. *J Biol Chem* 279:24053–24063.
- Tong AH, Evangelista M, Parsons AB, Xu H, Bader GD, Page N, Robinson M, Raghibzadeh S, Hogue CW, Bussey H, Andrews B, Tyers M, Boone C. 2001. Systematic genetic analysis with ordered arrays of yeast deletion mutants. *Science* 294:2364–2368.
- Tong AH, Lesage G, Bader GD, Ding H, Xu H, Xin X, Young J, Berriz GF, Brost RL, Chang M, Chen Y, Cheng X, Chua G, Friesen H, Goldberg DS, Haynes J, Humphries C, He G, Hussein S, Ke L, Krogan N, Li Z, Levinson JN, Lu H, Menard P, Munyana C, Parsons AB, Ryan O, Tonikian R, Roberts T, Sdicu AM, Shapiro J, Sheikh B, Suter B, Wong SL, Zhang LV, Zhu H, Burd CG, Munro S, Sander C, Rine J, Greenblatt J, Peter M, Bretscher A, Bell G, Roth FP, Brown GW, Andrews B, Bussey H, Boone C. 2004. Global mapping of the yeast genetic interaction network. *Science* 303:808–813.
- Tse E, Smith AJ, Hunt S, Lavenir I, Forster A, Warren AJ, Grutz G, Feroni L, Carlton MB, Colledge WH, Boehm T, Rabbitts TH. 2004. Null mutation of the Lmo4 gene or a combined null mutation of the Lmo1/Lmo3 genes causes perinatal lethality, and Lmo4 controls neural tube development in mice. *Mol Cell Biol* 24:2063–2073.
- Val P, Martinez-Barbera JP, Swain A. 2007. Adrenal development is initiated by Cited2 and Wt1 through modulation of Sf-1 dosage. *Development* 134:2349–2358.
- Weninger WJ, Floro KL, Bennett MB, Withington SL, Preis JI, Barbera JP, Mohun TJ, Dunwoodie SL. 2005. Cited2 is required both for heart morphogenesis and establishment of the left-right axis in mouse development. *Development* 132:1337–1348.
- Withington SL, Scott AN, Saunders DN, Lopes Floro K, Preis JI, Michalick J, Maclean K, Sparrow DB, Barbera JP, Dunwoodie SL. 2006. Loss of Cited2 affects trophoblast formation and vascularization of the mouse placenta. *Dev Biol* 294:67–82.
- Wong SL, Zhang LV, Tong AH, Li Z, Goldberg DS, King OD, Lesage G, Vidal M, Andrews B, Bussey H, Boone C, Roth FP. 2004. Combining biological networks to predict genetic interactions. *Proc Natl Acad Sci U S A* 101:15682–15687.
- Xu PX, Zheng W, Laclef C, Maire P, Maas RL, Peters H, Xu X. 2002. Eya1 is required for the morphogenesis of mammalian thymus, parathyroid and thyroid. *Development* 129:3033–3044.
- Yin Z, Haynie J, Yang X, Han B, Kiatchoosakun S, Restivo J, Yuan S, Prabhakar NR, Herrup K, Conlon RA, Hoit BD, Watanabe M, Yang YC. 2002. The essential role of Cited2, a negative regulator for HIF-1alpha, in heart development and neuroulation. *Proc Natl Acad Sci U S A* 99:10488–10493.
- Zhang Z, Baldini A. 2007. In vivo response to high-resolution variation of Tbx1 mRNA dosage. *Hum Mol Genet* 17:150–157.
- Zou D, Silvius D, Davenport J, Grifone R, Maire P, Xu PX. 2006. Patterning of the third pharyngeal pouch into thymus/parathyroid by Six and Eya1. *Dev Biol* 293:499–512.